Optical Properties of Erbium Doped Lead Bismuth Borate Glasses

V Manju[1], K Krishna Murthy Goud[2], B Appa Rao[1]

[1]Department of Physics, Univ. College of Engineering Science and Technology, JNTUH, Hyderabad, Telangana (India)
[2]Department of Physics, Univ. College of Engineering, Osmania University, Hyderabad, Telangana (India)

***

Abstract – Erbium doped lead bismuth borate glasses with the composition$60PbO-20B_2O_3-(20-x)Bi_2O_3-xEr_2O_3$; where $x = 0$, 0.5 and 1.0 mol% have been prepared by melt quenching technique. Structural and optical properties of the prepared samples were studied using X-ray diffraction (XRD), Optical absorption spectroscopy and FTIR spectroscopy. XRD studies confirmed the amorphous nature of the prepared glass samples. Optical absorption studies showed presence of various absorption bands attributed to 4f-4f transitions of Er^{3+} ions from the ground ($^4I_{15/2}$) state to the excited states at 488 nm ($^4F_{7/2}$), 521 nm ($^2H_{11/2}$), 545 nm ($^4S_{3/2}$), 652 nm ($^4F_{9/2}$), 798 nm ($^4I_{9/2}$), 980nm ($^4I_{11/2}$) and 1510 nm ($^4I_{13/2}$). FTIR spectra revealed the presence of PbO_4, BO_3 and BO_4 units in PBBE glasses are evident from infrared spectral studies

***Key Words*:**Glasses, XRD, Optical absorption, and FTIR

1.INTRODUCTION

Since about 40 years, rare earth ions like Er^{3+} have attracted much interest as luminescence centers in crystals as well as in glasses [1 ,2]. Presently, special attention is paid to erbium due to its emission band at 1.53 µm which makes it an ideal element for applications in the field of optical data transmission (erbium-doped fiber amplifier). In all trivalent RE activator ions Er^{3+} is widely popular owing to its NIR emissions at ~0.85 mm($^4S_{3/2}/^4I_{13/2}$), ~1.25 mm ($^4S_{3/2}/\ ^4I_{11/2}$), ~1.53 mm ($^4I_{13/2}/\ ^4I_{15/2}$), and ~1.7 mm ($^4S_{3/2}/\ ^4I_{9/2}$), and MIR emissions at ~2.8 mm ($^4I_{11/2}/^4I_{13/2}$), ~3.3 mm ($^4S_{3/2}/4F_{9/2}$), and ~3.5 mm ($^4F_{9/2}/\ ^4I_{9/2}$) including upconversion luminescence at ~0.66 mm ($^4F_{9/2}/^4I_{15/2}$), ~0.55 mm ($^4S_{3/2}/\ ^4I_{15/2}$), and ~0.525 mm ($^2H_{11/2}/\ ^4I_{15/2}$) [3].

In all distinct kinds of oxide glasses, borate is familiar as a typical network former owing to its favorable traits like large glass formation tendency, lesser fusion heat, higher bond strength, better thermal and mechanical stabilities, small cation size, reasonable RE ion's solubility, and better optical transparency [4, 5]. In recent times, glasses containing heavy metal oxide network formers doped with luminescent lanthanide ions have attracted a considerable interest due to their low vibrational frequencies [6], which cause the non-radiative relaxation from the exited states of the dopant ions to be inefficient 70]. This can lead to interesting applications for the development of optical devices requiring high emission quantum yields, such as solid-state lasers and optical amplifiers [8]. On the other hand, glasses containing heavy metal oxide network formers and/or modifiers exhibit interesting non-linear optical properties. After optical/thermal poling we can find applications for NLO devices. In the case of Ln^{3+} doped materials, these properties could lead to the possible development of self-frequency-doubling lasers.

In this investigation, lead bismuth borate glasses doped with erbium ions have been prepared. The XRD, optical absorption and FTIR spectra have been measured for the prepared samples and the results are discussed in detail.

2. EXPERIMENTAL

For the present study, glasses with the composition $60PbO-20B_2O_3-(20-x)Bi_2O_3-xEr_2O_3$; where $x = 0$, 0.5 and 1.0 mol% are chosenand the glass samples are labelled as PBBE0, PBBE0.5 and PBBE1, respectively. Appropriate amounts of AR grade reagents of PbO, H_3BO_3, Bi_2O_3 and Er_2O_3 powders were weighed by using digital electronic balance. All the glass samples were prepared by conventional melt quenching technique.

The X-ray diffraction (XRD) spectra for all the glass samples were recorded using Rigaku MiniFlextable top X-ray diffractometer. The optical absorption spectra were obtained with the Perkin Elmer lambda 950 UV-VIS-NIR spectrophotometer at 350–2000 nm spectral span. The FTIR spectra of glass samples were recorded on a BRUKER OPTICS, TENSOR-27 infrared spectrometer in the range 4000 - 400 cm^{-1}. For IR measurements, the glasses were pulverized and mixed with KBr in order to obtain thin pellets with a thickness of about 0.3mm.

3. RESULTS AND DISCUSSION

X-Ray Diffraction

The X-ray diffraction spectra of all the prepared samples is shown in Fig. 1. The samples prepared were free from visible inhomogeneities, such as inclusions, cracks or bubbles. The diffraction patterns obtained have proved the vitreous character of these samples.

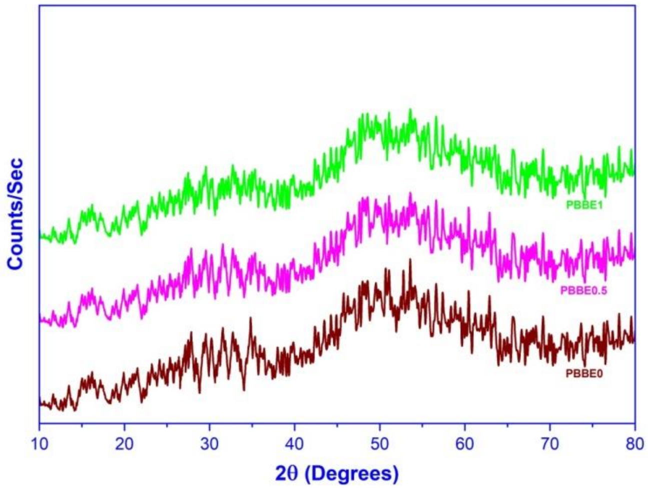

Fig-1:XRD diffractograms of PBBE glasses.

Optical absorption

Fig .2 depicts UV-Vis-NIR absorption spectra of prepared glass samples at 350–2000 nm spectral span.The spectra exhibited six absorption bands attributed to 4f-4f transitions of Er^{3+} ions from the ground ($^4I_{15/2}$) state to the excited states at 488 nm ($^4F_{7/2}$), 521 nm ($^2H_{11/2}$), 545 nm ($^4S_{3/2}$), 652 nm ($^4F_{9/2}$), 798 nm ($^4I_{9/2}$), 980nm ($^4I_{11/2}$) and 1510 nm ($^4I_{13/2}$) [9, 10].

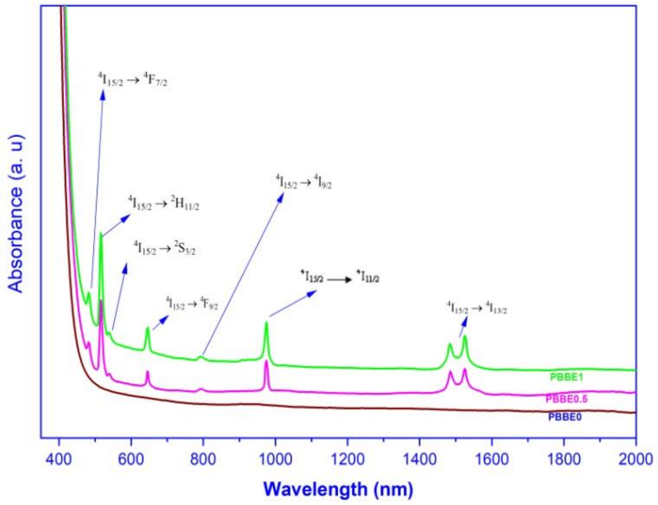

Fig-2: Optical absorption spectra of PBBE glasses.

The transition energies obtained in the present glasses are similar to those measured in other glasses. The intensities of all bands were found to increase with increase in the concentration of Er^{3+} ions. There is no significant shift is observed in the band positions. Here $^4I_{15/2} \rightarrow {}^4I_{13/2}$ transition shows both MD (magneticdipole) and ED (electric-dipole) contributions, and the rest of them all are ED only in nature. Moreover, in all transitions, $^4I_{15/2} \rightarrow {}^2H_{11/2}$ are proportionally very intense as they obey $\Delta S=0$, $|\Delta L| \leq 2$, and $|\Delta J| \leq 2$ selection rule as HS (hypersensitive) ones [11-13]. Usually, such HS transitions intensity varies considerably depending on Er^{3+} ion's interaction strength with host matrix in a local environment that ultimately affects $\Omega_{2,4,6}$ (J-O parameters) magnitude.

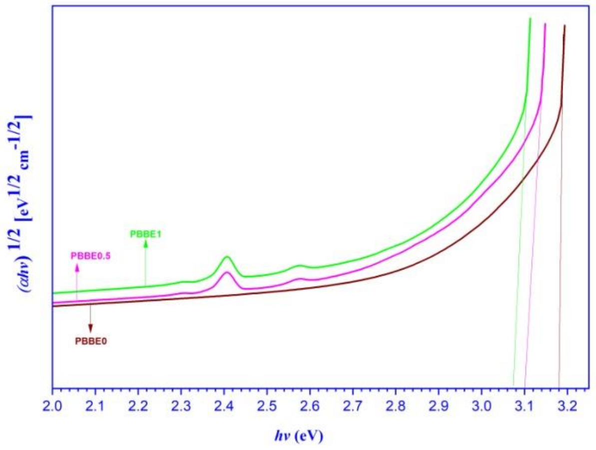

Fig-3: The $(\alpha h\nu)^{1/2}$ as a function of photon energy for the PBBE glasses.

From the spectra it was observed that cut-off wavelength value increased with the addition of Er_2O_3. The absorption coefficient 'α' below and near the fundamental absorption edge of each curve in Fig. 2 was determined, from the relation [14]

$$\alpha(\omega) = \left(\frac{1}{t}\right)\ln\left(\frac{I}{I_0}\right) \quad \ldots\ldots\ldots\ldots\ldots\ldots\ldots.. (1)$$

where '*t*' is the thickness of each sample and *ln (I/I₀)* corresponds to absorbance. Thus the data for Fig. 3 were obtained from the relation [15]

$$\alpha(\omega) = const.\left(h\nu - E_{opt}\right)^2 / h\nu \quad \ldots\ldots\ldots\ldots\ldots\ldots.. \quad (2)$$

where E_{opt} is the energy of the optical band gap and '$h\nu$' is the photon energy of the incident radiation. Since relation (2) can be readjusted to represent the linearity between $(\alpha h\nu)^{1/2}$ and $(h\nu\text{-}E_{opt})$, one can determine the optical band gap values from the curves representing $(\alpha h\nu)^{1/2}$ as a function of the photon energy ($h\nu$) shown in Fig. 3.Thus the data obtained from Fig. 3.2 were fitted to the equation

$$(\alpha h\nu)^{1/2} = const.\left(h\nu - E_{opt}\right) \quad \ldots\ldots\ldots\ldots\ldots\ldots.. (3)$$

for the linear regions of the curves in Fig. 3 by the method of least squares. The E_{opt}values were determined by extrapolation of the linear region of the plots of $(\alpha h\nu)^{1/2}$ against$h\nu$ to $(\alpha h\nu)^{1/2} = 0$. The values of E_{opt} obtained are given in Table 1.

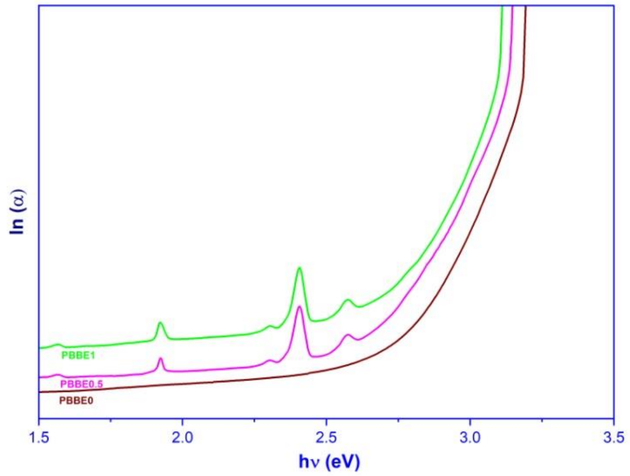

Fig-4: The ln (α) as a function of photon energy for the PBBE glasses.

The logarithm of the absorption coefficient 'α' was plotted as a function of the photon energy ($h\nu$) for various compositions of the glasses (Fig. 4). The values of the Urbach energy (ΔE) were calculated by taking the reciprocals of the slopes of the linear portion in the lower photon energy region of these curves. The values of ΔE for different compositions are given in Table 1.

From the values presented in Table 1, it was observed that the decrease of optical band gap (E_{opt}) and increase in Urbach energy takes place with the addition of Er_2O_3. The presence of Er_2O_3 is likely modifying the structure of the glass, improving the connection between boron-oxygen tetrahedra or other structural components. As a modifier, Er^{3+} ions increase the concentration of non-bridging oxygens (NBOs) by creating dangling bonds [16-19]. Such defects increase the degree of localization of electrons, thereby increasing the donor centers in the glass matrix. The presence of large concentration of these donor centers lowers the optical band gap and shifts the absorption edge towards high wavelength side as observed. Probably in this concentration range the erbium ions may take network forming positions with ErO_4 structural units and alternate with BO_4 units. Such linkages may cause a decrease in the rigidity of the glass network and leads to the decrease in the optical band gap and increase in the Urbach energy as observed. The increase in Urbach energy is indicative of an increase in concentration of NBOs and disorder in the glass network.

Table-1: Values of cut off wavelength, optical band gap and Urbach energy of PBBE glasses.

S.No.	Sample code	Cut-off wavelength (nm)	E_{opt}(eV) ±0.01	ΔE (eV) ±0.001
1	PBBE0	390	3.18	0.134
2	PBBE0.5	400	3.10	0.139
3	PBBE1	407	3.07	0.142

Urbach energy that is generally interpreted as the width of tail of energy levels in the optical energy gap and is found to increase with temperature. Highly crystalline solids show a very sharp absorption edge with small ΔE values. Therefore, Urbach energy can be considered as a measure of disorder in amorphous and crystalline materials [19-21]. The higher the concentration of NBOs in the glass network, the smaller the optical energy gap and the greater are the Urbach energy values in borate glasses [22]. The increase in the Urbach energy is indicative of an increase in concentration of NBOs and disorder in the glass network.

FTIR

Fig. 5 shows the FTIR spectra of lead bismuth borate glasses doped with erbium ions in the range 1600-400 cm^{-1}.The FTIR spectra of PBBE glass system shows characteristic bands corresponding to the different vibration modes of the various functional groups present in the glass system.

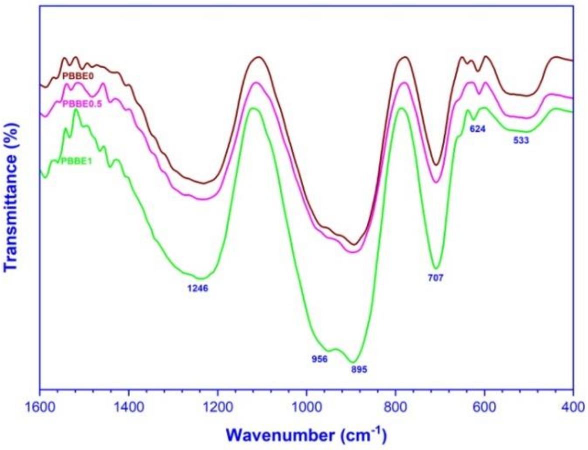

Fig-5: FTIR spectra of PBBE glasses.

Previous research reported that the transmission band of borate network is mainly active in only three spectral regions [23, 24]. The first band of borate network is located in the range of 1200–1600 cm^{-1}. This correlates with the asymmetric stretching vibration of the B-O band in trigonal BO_3 units [25]. The second band of borate network lies in the range of 800–1200 cm^{-1} which corresponds to the stretching vibrations of B-O band in tetrahedral BO4 units. The third group of borate network is positioned in the range of 700 cm^{-1} which correlates to bending vibrations of B-O-B in trigonal BO_3 units.

The FTIR spectra of lead bismuth borate glasses doped with erbium ions reveals the presence of active peaks around 533, 615, 709, 896, 956 and 1246 cm^{-1}. The band at ~533 cm^{-1} can be attributed to the Bi-O bending vibration in BiO_6 units [26] and also due to the presence of PbO_4 structural units [27]. The peak at 612 cm^{-1} is observed to be in the glass, which can be attributed to stretching vibrations of Bi–O bonds in BiO_6 [28, 29] and also may be due to the presence of ErO_4 bending modes (Er– *O*–Er) [44].

Table-2: Absorption bands and their assignments for FT-IR spectra.

Wave number (cm^{-1})			IR assignments
PBBE0	PBBE0.5	PBBE1	
~533	~533	~533	Due to the Bi-O bending vibration in BiO_6 units.
~612	~612	~624	Due to the ErO_4 bending modes (Er– *O*–Er)
~709	~709	~707	Due to the bending vibration of B–O–B linkages in the borate network and vibrations of PbO_4 groups can also be associated with this band.
~895 ~956	~897 ~956	~896 ~956	Due to the B-O stretching vibration in BO_4 units from di-borate groups and also this band may be due to vibration of strongly distorted BiO_6 octahedral units.
~1246	~1246	~1246	Due to the B–O asymmetric stretching vibrations in BO_3 unit from pyro- and ortho-borate groups.

Many authors suggested that Bi_2O_3 in Bi_2O_3-B_2O_3 glasses can share in the structure in three different ways; it gives part of its oxygen to the boron to create a four coordinated state; it participates in the structure by forming BiO_3 groups belonging to the pyramidal point group C_{3v}; and it introduces some nonbridging oxygens. It was shown that Bi_2O_3 appears in the glass networks as deformed BiO_6 units [30-31], both BiO_6 and BiO_3polyhedra [32] or only as BiO_3 pyramidal units [33]. The most important condition for the existence of BiO_3 polyhedra is the presence of a band at 830 cm^{-1} in the FTIR spectra [31, 32]. The absence of this band in the FTIR spectra of the present glasses proves that Bi^{3+} cations are incorporated in the structure of glasses as only BiO_6 octahedral units.Rare earth doped bismuth borate glasses present a relatively high rigidity of the vitreous host glass matrix. Thus, the presence of RE ions in the glass composition seems to influence the surrounding of the Bi^{3+} cations favoring the formation of the BiO_3 units. The Bi^{3+} cations are incorporated in the network of these glasses as BiO_6 units, while the boron atoms takes part in the glass network as BO_3 and BO_4 units [34-36].

The band at ~709 cm^{-1} is due to bending vibration of B–O–B linkages in the borate network and vibrations of PbO_4 groups can also be associated with this band [37, 38]. The B-O stretching vibration in BO_4 units from di-borate groups was observed at ~896, ~956 cm^{-1} [39] and also this band may be due to vibration of strongly distorted BiO_6 octahedral units [26, 27]. The absorption band at ~1246 cm^{-1} was assigned to B–O asymmetric stretching vibrations in BO_3 unit from pyro- and ortho-borate groups [40, 41].

In borate glass, B_2O_3, possesses boroxyl ring structural arrangement located at 806 cm^{-1}.However, this band disappeared after the glass formation which indicates the absence of boroxyl ring in the glass system. Furthermore, the trigonal BO_3 and tetrahedral BO_4 are taking place after the glass formation [43]. This is in agreement with the IR spectroscopy results, which detected a decrease in the intensity for four coordinated boron atoms BO_4 than those three-coordinated ones of BO_3 with increasing Er_2O_3 concentration. The decrease of the BO_4 groups with the addition of erbium oxide depends on the number of oxygen atoms and converted BO_4 to BO_3 groups and forms non-bridging oxygen (NBO). In addition, erbium oxide may enter the network as a modifier, which affects the probability of BO_4 formation, i.e. increase of Er_2O_3 concentration breaking up tetrahedral bonds of BO_4 units and introduce coordination defects known as dangling bonds [41, 42].

4. CONCLUSIONS

Optical properties of erbium doped lead bismuth borate glasses were studied. The X-ray diffraction (XRD) spectra of the glass samples show absence of sharp peaks. The absence of sharp peaks confirms the amorphous nature of the prepared glass samples. FTIR spectra of the base glass and RE-doped glasses exhibit significantly characteristic vibrational bands due to combined vibrations of borate network and Bi–O vibrations. FTIR spectra revealed the presence of the various functional groups in the prepared glasses.Absorption spectra showed distinct extended Er^{3+} ion’s bands from UV to NIR region.

The values of ΔE are consistent with the trend of E_{opt} values. The variations in the values of E_{opt} and ΔE can be understood in terms of the structural changes that are taking place in glass samples. The value of optical band gap (E_{opt}) reduced with increase in the concentration of Er^{3+} ions specifying higher NBOs creation over BOs in the glass structure. Overall, these results indicate that the studied glasses are potential candidates for laser and broadband amplifiers.

REFERENCES

1. Snitzer, E.,Woodcock, R.F.: *J. Opt. Soc. Am.* **55** (1965) 608.
2. Snitzer, E.,Woodcock, R.F.:*J. Segre, IEEE J. Quantum Electron* **QE 4** (1968) 360.
3. He H, Jia, Z., Wang, T., Ohishi, Y., Qin, W., Qin, G.:*Opt Lett* 2021;46:1057:60.
4. Bengisu, M.:*J Mater Sci* 2016;51:2199:242.
5. Eigen, M.: Chapter 12 - OXIDE GLASSES. In: Rao KJ, editor. Structural chemistry of glasses. *Elsevier Science Ltd*; 2002,ISBN 9780080439587. p. 463e511.
6. Wachtler, M.,Speghini, A.,Gatterer, K.,Fritzer, H.P.,Ajo D.,Bettinelli,M.:*J. Am. Ceram. Soc.* **81** (1998) 2045.
7. Layne, C.B.,Lowdermilk,W.H.,Weber, M.: J. *Phys. Rev. B***16** (1977)10.
8. Ebendorff-Heidepriem,H.,Ehrt, D.,Bettinelli, M.,Speghini, A.,Jiang,S., Hokkanen,S.:(Eds.), *SPIE Proceedings*, vol. **3622**, 1999, p. 19.
9. Caetano, M., Silva, A.C.A., Filho, J.C.S., de Morais, R.F., Sales, T.O., Andrade, A.A.:*J Lumin* 2020;228:117599.
10. Deopa, N., Sahu, M.K., Kaur, S., Prasad, A., Swapna, K., Kumar, V.: *J Rare Earths* 2021;39:520:5.
11. Lakshminarayana, G., Meza-Rocha, A.N., Soriano-Romero, O., Huerta, E.F., Caldino, U., Lira, A.:*J Mater Res Technol* 2021;13:2501:26.
12. Lakshminarayana, G., Meza-Rocha, A.N., Soriano-Romero,.O, Huerta, E.F., Caldino, U., Lira, A.:*J Alloys Compd*2021;884:161076.
13. Lakshminarayana G, Meza-Rocha AN, Soriano-Romero O, Huerta EF, Caldino U, Lira A, *Results Phys* 2021;26:104343.
14. Sands,R.H.:*Phys. Rev.* **99** (1995) 1222.
15. Davis,E.A.,Mott,N.F.: *Phil. Mag.* **22** (1970) 903.
16. Sun, J.,Zhang, J.,Luo, Y.,Lu, S., Ren, X., Chen, B., Wang, X.:*Opt. Mater.* **28** (2006) 306–309.
17. Liu, X.,Zhang, C., Wu, S.,Liu, Y.:*Ceram. Int.* **49** (2023) 38115–38121.
18. Urbach,F.: *Phys. Rev.***92** (1953) 1324.
19. Redfield,D.: *Phys. Rev.***130** (1963) 916.
20. Dexter,D.L.: *Phys. Rev. Lett.***19** (1967) 1383.
21. Sheibani,R.D.,Hogarth,C.A.: *J. Mater. Sci.***26** (1991) 429.
22. Pascuta,P., Borodi, G.,Culea, E.: *J. Non-Cryst. Solids* **354** (2008) 5475
23. Karthikeyan, B.,Philip, R.,Mohan, S.: *Optics Communications* **246**, no. 1–3 (2005) 153–162.
24. Karthikeyan,B.,Mohan, S.: *Physica B: Condensed Matter* **334** (2003) 298–302.
25. Farouk, M., Samir, A., Metawe, F., Elokr,M.: *Journal of Non-Crystalline Solids*, **vol. 371-372** (2013), pp. 14–21.
26. Hu, Y.,Liu, N.H.,Lin, U.L.:*J. Mater. Sci.***33**, 229 (1998).
27. Veerabhadra Rao, A.,Laxmikanth, C.,Appa Rao,B.,Veeraiah, N.: *J. Phys. Chem. Solids* **67** (2006) 2263.
28. Rajyasree, C.,Rao, D.K.: *J. Non-Cryst. Solids* **357** (2010) 836–841.
29. Simon, V.,Srinu, M.,Stefan, R.:*J. Mater. Sci: Mater. Med.* **18** (2007) 507.
30. ElBatal, F.H.,Marzouk, S.Y.,Nada, N.,Desouky, S.M.: *Physica B* **391**, 88 (2007).
31. Iordanova, R.,Dimitrov, V.,Dimitriev, Y.: *J. Non- Cryst. Solid s***180**, 58 (1994).
32. El Batal, F.H.,Marzouk, S.Y.,Nada, N.,Desouky, S.M.:*Physica B* **391**, 88 (2007).
33. AzlanMuhammadNoorazlan, Halimah Mohamed Kamari, Sharudin Omar Baki, Daud W.Mohamad:*Journal of Nanomaterials* Volume 2015, Article ID 952308, 9 pages.
34. Dexter, D.L.:*Phys. Rev. Lett.***19** (1967) 1383.
35. Baia, L.,Stefan,R., Popp, J.,Simon, S.,Kiefer, W.: *J.Non-Cryst. Solids* **324**, 109 (2003).
36. El-Egili, K.:*Physica B* **325**, 340 (2003).

37. Manisha pal, A., Hirota, K., Tsujigami, Y., Sakata, H.:*J Phys D: Appl Phys* 2001;34:459.
38. Sherief, M., Abo-Naf:*J. Non-Cryst. Solids* **358** (2012) 406–413,http://dx.doi.org/ 0.1016/j.jnoncrysol.2011.10.013
39. Kumar, A., Rai, S.B., Rai, D.K.:*Mater Res Bull* 2003;38:333.
40. Yiannopoulos, Y.D., Chryssikos, G.D., Kamitsos,E.I:.*Phys Chem Glasses* (2001);42:424.
41. Pascuta, P., Pop, L., Rada, S., Bosca, M., Culea, E.:*J Mater Sci Mater Electron* 2008;19(5):424.
42. Kishan Murthy, M., Murthy, K.S.N., Veeraah, N.:*Bull Mater Sci* 2002;23(4).
43. Maniu, D., Iliescu, I., Cinta, S., cozar, O.:*J Mol Struct* 1997;410-411:291–4.
44. Wu, J.,Li, Y.,Zhao, Y.,Wu, C., Li, Z.,Lu,A.:*J. Non-Cryst. Solids* **583** (2022) 121469.